

## pH-Dependent Configurations of a 5-Chlorouracil-Guanine Base Pair<sup>†</sup>

Jacob A. Theruvathu, Cherine H. Kim, Agus Darwanto, Jonathan W. Neidigh, and Lawrence C. Sowers\*

*Department of Basic Sciences, School of Medicine, Loma Linda University, Loma Linda, California 92350*

*Received July 7, 2009; Revised Manuscript Received September 22, 2009*

**ABSTRACT:** Hypochlorous acid (HOCl) from activated neutrophils at sites of inflammation can react with and damage biological molecules, including nucleic acids. The reaction of HOCl with cytosine analogues can generate multiple products, including 5-chlorouracil (CIU). In this paper, we have constructed oligonucleotides containing CIU paired opposite guanine (CIU-G). Melting studies indicate that oligonucleotide duplexes containing the CIU-G mispair are substantially less stable than those containing a CIU-A base pair. The melting temperature of the CIU-G mispair is not experimentally distinguishable from that of a T-G pair. NMR studies indicate that the CIU-G base pair adopts a wobble geometry at neutral pH, similar to a T-G mispair. The exchangeable protons of the CIU-G mispair broaden rapidly with an increase in temperature, indicating that the CIU-G mispair is less stable and opens more easily than the surrounding adjacent base pairs. Unlike the CIU-A base pair studied previously [Theruvathu, J. A., et al. (2009) *Biochemistry* *48*, 7539–7546], the CIU-G mispair undergoes a pH-dependent structural change, assuming an ionized base pair configuration that approximates a Watson–Crick base pair at higher pH. Ionization of CIU in a DNA template could promote mispair formation and mutation, in accord with previous studies on other 5-halouracil analogues. The electron-withdrawing 5-chloro substituent facilitates ionization of the CIU N3 proton, promoting mispair formation, but it also renders the glycosidic bond susceptible to base cleavage by DNA repair glycosylases.

Reactive molecules generated by cells of the innate immune system, including neutrophils and eosinophils, are known to react with lipids, proteins, and nucleic acids (1–5). While highly reactive molecules, including hypochlorous acid (HOCl),<sup>1</sup> have potent antimicrobial activity, these reactive species can also cause collateral damage to host molecules. Emerging evidence indicates that HOCl-mediated damage is frequently found at sites of inflammation, suggesting a potential connection between inflammation and the development of human disease, including cancer (6).

The reaction of HOCl with cytosine generates an array of products (7), including 5-chlorocytosine (CIC) and 5-chlorouracil (CIU). If the initial reaction occurred with a cytosine residue in a G–C base pair, the result could be a CIU–G mispair (Figure 1a). Base pairs in DNA containing CIU can also result from the incorporation of CIU-containing nucleotides generated by the reaction of HOCl with nucleotide pools (8–11).

In a recent study, we examined the configuration and stability of a base pair containing CIU paired with adenine in a model synthetic oligonucleotide duplex (12). The configuration of the

CIU–A base pair was similar to that of a normal T–A base pair; however, it was slightly more thermally and thermodynamically stable. The line width of the CIU imino proton did not increase with an increase in solution pH. Although the CIU imino proton is more acidic than the corresponding thymine (T) imino proton, the absence of pH-dependent line broadening at pH values well above the pK<sub>a</sub> of CldU (5-chloro-2'-deoxyuridine) was attributed to the formation of a stronger hydrogen bond with the opposing adenine residue and an indicator that the N3 proton was needed for the formation of the CIU–A base pair. The inability of a repair glycosylase to remove CIU when paired with A was attributed to the apparent stability of the CIU–A base pair, suggesting that CIU when paired with A might be a persistent lesion in DNA.

Previous studies have examined oligonucleotide duplexes containing analogous 5-fluorouracil (FU) and 5-bromouracil (BrU) mispairs with guanine. The FU–G (13) and BrU–G (14) mispairs have been shown to be in a wobble geometry at neutral pH both by NMR and, in the case of BrU–G, by crystallography in a duplex that assumed a Z-DNA structure (15). With an increase in pH, the FU–G and BrU–G mispairs were shown to undergo a pH-dependent transition with formation of an ionized base pair in a geometry that approximated a Watson–Crick base pair (13, 14). The capacity of the halouracil–G mispairs to undergo a pH-dependent transition was attributed to the electron withdrawing property of the 5-halo substituent, which is the opposite of that of the thymine 5-methyl group. Subsequent studies from the Goodman laboratory (16) demonstrated that the degree of mispairing of the halouracil could be increased with an increase in solution pH, consistent with the ionized base pair model (17, 18).

The pK<sub>a</sub> values of the 2'-deoxynucleoside analogues of FU, CIU, BrU, and thymine are 7.7, 7.9, 8.0, and 9.7, respectively

<sup>†</sup>This work is supported by grant (GM41336) from the National Institutes of Health.

\*To whom correspondence should be addressed. Telephone: (909) 558-4480. Fax: (909) 558-4035. E-mail: lsowers@llu.edu.

Abbreviations: HOCl, hypochlorous acid; CIC, 5-chlorocytosine; CIU, 5-chlorouracil; CldU, 5-chloro-2'-deoxyuridine; DMT, dimethoxytrityl; GC–MS, gas chromatography–mass spectrometry; MALDI–TOF–MS, matrix-assisted laser desorption ionization time-of-flight mass spectrometry; DSS, 4,4-dimethyl-4-silapentane-1-sulfonate; T<sub>m</sub>, melting temperature; EDTA, ethylenediaminetetraacetic acid; NOE, nuclear Overhauser effect; FU, 5-fluorouracil; BrU, 5-bromouracil; TTP, thymidine triphosphate; dUTP, 2'-deoxyuridine 5'-triphosphate; UNG, uracil–DNA glycosylase; SMUG1, single-strand selective monofunctional uracil–DNA glycosylase; TDG, thymine–DNA glycosylase.

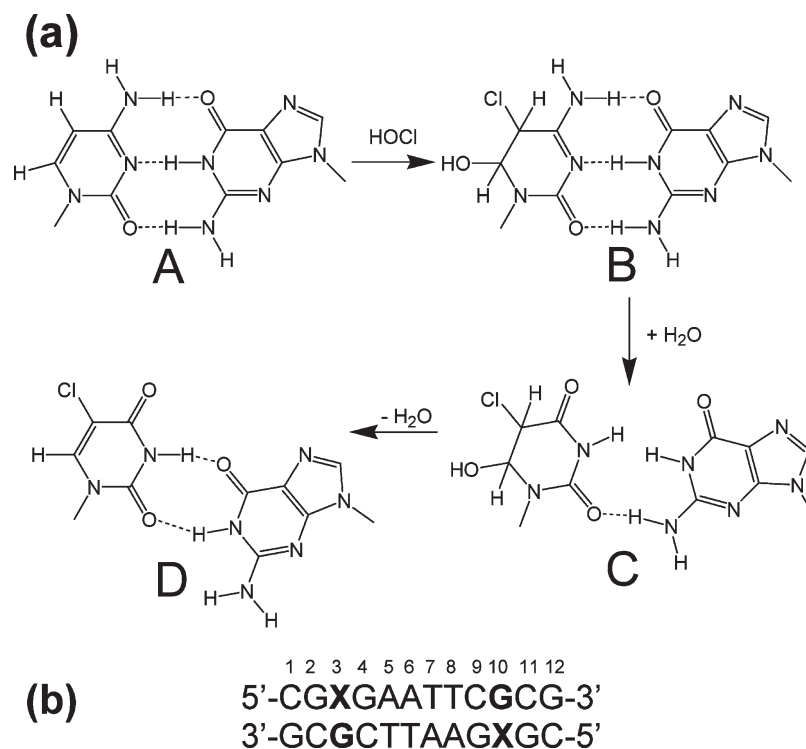


FIGURE 1: (a) Pathway for HOCl-mediated conversion of a C-G base pair to a CIU-G mispair. (A) Normal C-G base pair. (B) Dihydrocytosine intermediate formed from the addition of HOCl to cytosine. (C) Conversion of dihydrocytosine to dihydrouracil intermediate. (D) CIU-G mispair formed by dehydration. (b) The 12mer oligonucleotide used for the study, where X is 5-chlorouracil.

(19, 20). The 5-chloro substituent, like the analogous fluoro and bromo substituents, facilitates ionization of the pyrimidine ring N3 proton and destabilizes the glycosidic bond, promoting glycosylase repair (21–26). Although FU and BrU are similar with respect to the inductive properties of the 5-substituent, the biological properties are distinct. Derivatives of FU are highly toxic (27, 28). BrU is mutagenic, although mammalian cell grown in culture can tolerate substantial substitution of T with BrU (29, 30).

The distinct properties of FU and BrU are likely due in part to the size of the 5-substituent. The smaller size of fluorine allows 5-fluoro-2'-deoxyuridine 5'-monophosphate to mimic 2'-deoxyuridine 5'-monophosphate and poison thymidylate synthase. When in DNA, FU is also readily removed by all members of the uracil-glycosylase family of repair enzymes (21–26). In contrast, BrU can replace T in facilitating the binding of sequence-specific DNA–protein interactions (31, 32). BrU residues are repaired only by a subset of uracil glycosylases and usually only when mispaired with G (21–26).

The size of the 5-substituent of CIU is intermediate between fluorine and bromine, predicting that in some cases CIU would mimic FU but in other cases be more similar to BrU. Among the 5-halouracils, CIU would be the most likely formed under endogenous conditions. The incorporation of CIU into DNA is known to cause chromosomal aberrations, cellular senescence, and toxicity by as yet incompletely understood mechanisms (33–36). Recent studies indicating the formation of CIU as a byproduct of inflammation damage (1–6) bring new significance to understanding the properties of CIU. In this paper, we describe the results of studies with synthetic oligonucleotides in which CIU has been placed opposite G. We report the impact of this substitution on oligonucleotide stability and conformation.

## MATERIALS AND METHODS

**Oligonucleotide Synthesis.** Commercially available 2'-deoxyuridine was converted to CldU using the method of Kumar et al. (37). The corresponding phosphoramidite of CldU was prepared by standard methods, as previously described (36). All other phosphoramidites were obtained from Glen Research (Sterling, VA). Oligonucleotide synthesis was conducted with an Expedite synthesizer from Applied Biosystems (Foster City, CA). Oligonucleotides containing CldU were deprotected with concentrated aqueous ammonia at room temperature for 24 h.

The sequence of the 12mer oligonucleotide examined here is shown in Figure 1b. Oligonucleotides were purified by two rounds of HPLC, first with the dimethoxytrityl (DMT) group on and the second with the DMT group off. Oligonucleotides were examined by MALDI-TOF-MS (38), and the free base composition was verified by GC–MS following acid hydrolysis (39).

**Oligonucleotide UV Melting Studies.** The melting temperature ( $T_m$ ) and thermodynamic values of the oligonucleotide were obtained as previously described (40–42) using a Varian (Palo Alto, CA) Bio 300 Cary UV–vis spectrophotometer. The self-complementary oligonucleotide at various concentrations (2–60  $\mu$ M) was dissolved in a buffer containing 100 mM NaCl, 0.1 mM EDTA, and 10 mM sodium phosphate (pH 7). The sample was then treated with a thermal cycle from 10 to 90 °C at an interval of 0.5 °C. The thermodynamic values were obtained from the average of five such temperature cycles.  $T_m$  values are reported at a total strand concentration of 28  $\mu$ M (Table 1). Melting temperatures were also obtained from pH 7 to 11.

**Nuclear Magnetic Resonance Spectroscopy (NMR).** NMR spectra were obtained with a 500 MHz Bruker (Billerica, MA) NMR system. The proton NMR spectra of the oligonucleotide were recorded in a solution containing 10% D<sub>2</sub>O,

Table 1:  $T_m$  Values and Thermodynamic Parameters of the 5'-d(CGXGA-ATTCYCG)-3' (X = pyrimidine, Y = purine) Oligonucleotide in 10 mM Sodium Phosphate, 100 mM Sodium Chloride, and 0.1 mM EDTA (pH 7.0)<sup>a</sup>

	$T_m$ at 28 $\mu$ M (°C)	$\Delta H^\circ$ (kcal/mol)	$\Delta S^\circ$ (cal mol <sup>-1</sup> K <sup>-1</sup> )	$\Delta G^\circ$ (25 °C) (kcal/mol)
T-G	42.2 $\pm$ 0.2	-90.0 $\pm$ 3.7	-264 $\pm$ 12	-9.7 $\pm$ 0.2
CIU-G	41.8 $\pm$ 0.2	-86.7 $\pm$ 3.8	-254 $\pm$ 12	-9.5 $\pm$ 0.2
CIU-A	55.6 $\pm$ 0.3	-81 $\pm$ 14	-234 $\pm$ 4	-12.2 $\pm$ 1.0

<sup>a</sup>The values for CIU-A are from ref 12.

100 mM NaCl, 10 mM sodium phosphate, and 0.2 mM EDTA (pH 7.0) and compared with results for similar sequences published by other laboratories (43–45). The oligonucleotide (200  $A_{260}$  OD units, 2.5 mM) was annealed at 86 °C for 2 min and slowly cooled prior to acquisition of NMR spectra. Each spectrum was calibrated using DSS (4,4-dimethyl-4-silapentane-1-sulfonate) as an internal standard reference. Proton NMR spectra of oligonucleotides in 90% H<sub>2</sub>O were acquired with a water suppression double gradient echo WATERGATE W5 pulse program (46). The temperature of the sample was controlled by a variable-temperature monitor (Eurotherm, BVT 3000) from Bruker.

A typical spectrum was acquired with a binomial water suppression delay (d19) of 160  $\mu$ s which optimized water suppression. Since the delay (d19) of 160  $\mu$ s affected some of the imino resonances near 11 ppm, it was changed to 40  $\mu$ s when we examined the imino protons. The null point repetition was every 6.25 ppm from the suppression point when the d19 was 160  $\mu$ s. When the delay (d19) was 40  $\mu$ s, the null point repetition was far from any of the imino proton resonances. The line width studies were performed using a d19 delay of 40  $\mu$ s. The two-dimensional (2D) NOE spectra were acquired using a mixing time of 300 ms unless otherwise indicated.

## RESULTS

Commercially available 2'-deoxyuridine was converted to 5-chloro-2'-deoxyuridine (37) and then converted to the corresponding 5'-dimethoxytrityl-3'-cyanoethyl diisopropylamino-phosphoramidite (36). The phosphoramidite analogue of CIU was incorporated into a self-complementary synthetic oligonucleotide using standard solid phase methods. In the sequence prepared for this study, the CIU residue was paired opposite guanine (Figure 1b).

Oligonucleotides containing CIU were synthesized, deprotected, and purified using standard conditions, except that deprotection was conducted in concentrated aqueous ammonia at room temperature for 24 h. Because of the high natural abundance of both <sup>35</sup>Cl and <sup>37</sup>Cl isotopes, the mass spectrum of chlorine-containing molecules has a significant M + 2 line for the parent and M – methyl ions. Intact oligonucleotides were also examined by MALDI-TOF-MS. The isotope envelope of larger molecules can also be simulated (38); the presence of one chlorine atom in the oligonucleotide profoundly impacts the shape of the isotope envelope. The simulated ion cluster of an oligonucleotide with a composition of C<sub>116</sub>H<sub>145</sub>N<sub>45</sub>O<sub>71</sub>P<sub>11</sub>Cl matches the experimental spectrum (Figure S1a of the Supporting Information). The base composition of each oligonucleotide was verified by GC–MS following acid hydrolysis (Figure S1b of the Supporting Information).

The thermal stability of the oligonucleotide duplex (40–42) containing CIU was examined and compared with that of an

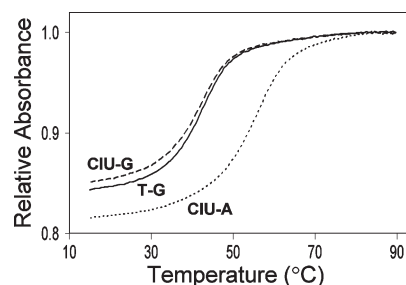


FIGURE 2: Oligonucleotide melting profiles examined by temperature-dependent absorbance at 260 nm. UV melting profiles (normalized) of the 12mer oligonucleotide at 28  $\mu$ M in a buffer containing 100 mM sodium chloride, 10 mM sodium phosphate, and 0.1 mM EDTA (pH 7.0): T-G (—), CIU-G (---), and CIU-A (···, from ref 12).

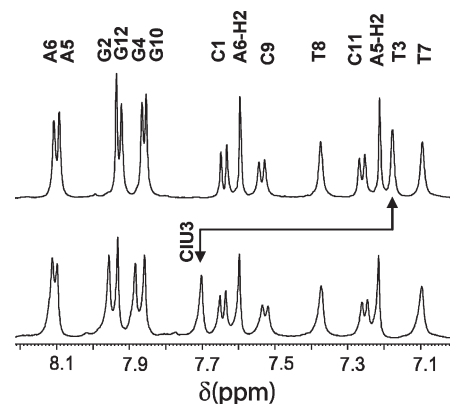


FIGURE 3: <sup>1</sup>H NMR spectra of the T-G (top) and CIU-G (bottom) oligonucleotides in the aromatic region. The H6/H8 and H2 assignments are written for the top spectrum. CIU3 of CIU-G oligo is indicated by the arrow in the bottom panel. The spectra were recorded at 27 °C with 256 scans using a water suppression WATERGATE program with a binomial water suppression delay (d19) of 160  $\mu$ s. The oligonucleotide was dissolved in a buffer containing 10% D<sub>2</sub>O, 100 mM sodium chloride, 10 mM sodium phosphate, and 0.2 mM EDTA (pH 7).

oligonucleotide containing T. The melting temperature at pH 7 of the oligonucleotide containing CIU-G was observed to be 41.8  $\pm$  0.2 °C, while that of the oligonucleotide containing T-G was 42.2  $\pm$  0.2 °C. Thermodynamic parameters obtained are listed in Table 1. The thermal melting profiles of the T- and CIU-containing oligonucleotides are shown in Figure 2.

Proton NMR spectra of the nonexchangeable protons of each duplex were obtained and are shown in Figure 3. Proton resonances were assigned by standard 2D methods (47), and assignments are provided in Table S1 of the Supporting Information. The corresponding 2D spectra for the duplexes containing the T-G and CIU-G mismatches are shown as Figures S2 and S3 of the Supporting Information. The observed proton connectivities indicate that both the T-G and CIU-G duplexes are predominantly in a B-form geometry and all bases are intrahelical. The H6 proton for T3 of the T-G oligonucleotide is observed at 7.18 ppm, whereas the corresponding H6 proton of the CIU residue of the CIU-G duplex is observed at 7.70 ppm.

Proton spectra of the exchangeable proton resonances were obtained in a 90% H<sub>2</sub>O/10% D<sub>2</sub>O mixture, and the spectra of the T-G and CIU-G duplexes are shown in Figure 4. Proton resonances were assigned by standard 2D methods, as described above. The 2D NOESY spectra of the exchangeable proton region for the T-G and CIU-G oligonucleotides are shown as

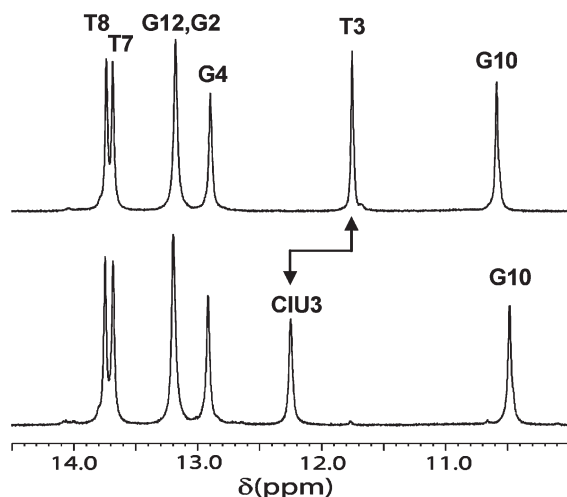


FIGURE 4:  $^1\text{H}$  NMR spectrum of the T-G (top) and CIU-G (bottom) oligonucleotides in the imino region. The spectra were recorded at 5  $^\circ\text{C}$  with 256 scans using a water suppression WATERGATE program with a binomial water suppression delay (d19) of 40  $\mu\text{s}$ . The oligonucleotide was dissolved in a buffer containing 10%  $\text{D}_2\text{O}$ , 100 mM sodium chloride, 10 mM sodium phosphate, and 0.2 mM EDTA (pH 6).

Figures S4 and S5 of the Supporting Information, respectively. The NOEs observed in Figures S4 and S5 between T3 and CIU3, respectively, and G10 imino protons are consistent with these mismatches being in a wobble base pair geometry. The resonance assignments are provided in Table S2 of the Supporting Information. The N3 imino proton of T3 of the T-G oligonucleotide was observed at 11.75 ppm and for CIU3 of the CIU-G oligonucleotide at 12.25 ppm. Other than chemical shift differences between protons in the T-G and CIU-G mismatches, all chemical shifts in the other base pairs were the same ( $\pm 0.02$  ppm).

The imino protons of the CIU-G mismatch broaden more rapidly with an increase in temperature than the corresponding imino protons of the T-G mismatch as shown in Figure 5. The one-dimensional (1D) spectra for the data plotted in Figure 5 are shown as Figures S6 and S7 of the Supporting Information. The magnitudes of the imino proton–water cross-peaks in the 2D NOESY spectra for the CIU-G mismatch are substantially greater than those for the T-G mismatch (Figure S8 of the Supporting Information). Potential base pair configurations are shown in Figure 6 and are discussed below.

With an increasing solution pH, the imino protons of the mismatched T-G and CIU-G bases broaden rapidly and are lost from the spectrum at pH 9 (Figure S9 of the Supporting Information).

The chemical shifts of nonexchangeable protons of bases above and below the mismatched CIU-G base pair move as a function of solution pH (Figure 7 and Figure S11 of the Supporting Information). The apparent midpoint of the pH-dependent transition for the CIU-G mismatch is approximately 8.75. As the pH increases, the G4 imino proton resonance shifts upfield from 12.95 to 12.45 ppm as the CIU-G base pair approaches pseudo-Watson–Crick geometry. A cross-peak is observed in the 2D NOESY spectrum at 12.45 and 12.95 ppm for the G4 imino proton due to chemical exchange (Figure S10 of the Supporting Information). No pH-dependent transition is observed for the T-G mismatch prior to alkaline denaturation of the helix. The observed melting temperatures of the CIU-A and CIU-G duplexes as a function of solution pH are shown in Figure 8.

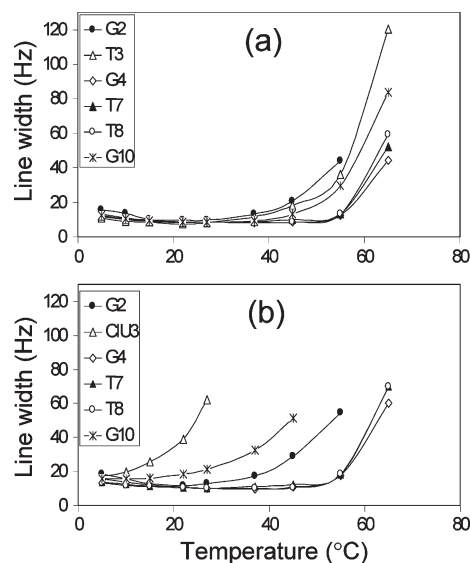


FIGURE 5: Line widths of imino protons as a function of temperature at pH 6: (a) T-G oligo and (b) CIU-G oligo. The spectra were recorded with 256 scans using a water suppression WATERGATE program with a binomial water suppression delay (d19) of 40  $\mu\text{s}$ . The oligonucleotide was dissolved in a buffer containing 10%  $\text{D}_2\text{O}$ , 100 mM sodium chloride, 10 mM sodium phosphate, and 0.2 mM EDTA.

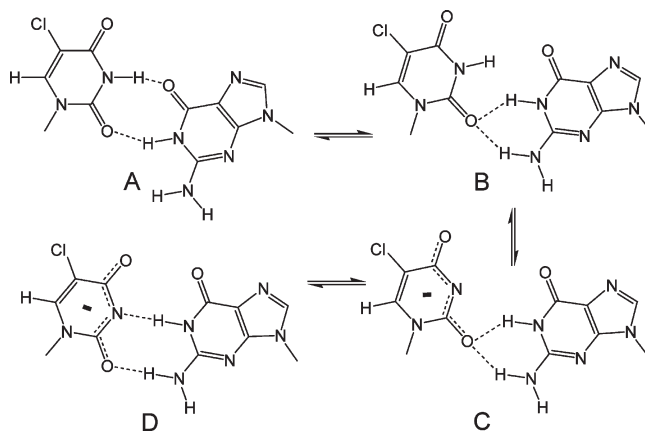


FIGURE 6: Possible base pairing configurations of the CIU-G mismatch.

No apparent change in helix thermal stability is observed in the region of the apparent  $\text{pK}_a$  of the CIU-G mismatch.

## DISCUSSION

DNA can be damaged by reactive molecules derived from activated neutrophils and eosinophils at sites of inflammation forming CIU and BrU, respectively (1–5, 30). Oxidized and halogenated pyrimidines, including CIU, are among the multiple damage products (Figure 1a). DNA damage products derived from reactive oxygen and halogen species might provide a mechanistic link between inflammation and human diseases, including cancer (6).

The 5-halogenated analogues of 2'-deoxyuridine can be metabolized to the triphosphate derivatives and incorporated into polynucleotides by polymerases. The FU analogues also serve as potent chemotherapy agents, in part because of their capacity to inhibit the synthesis of the normal DNA precursor, TTP (27, 28). While the halouracils are best known as synthetic analogues



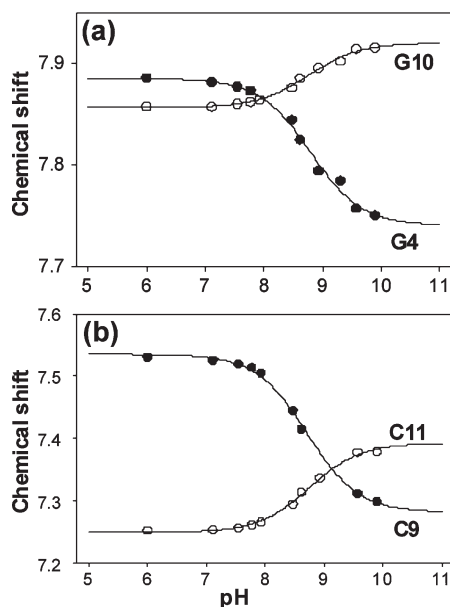


FIGURE 7:  $^1\text{H}$  NMR chemical shift study of the CIU-G oligo as a function of pH at room temperature. pH-dependent chemical shifts of (a) H8 protons of G4 and G10 and (b) H6 protons of C9 and C11. The oligonucleotide was dissolved in a buffer containing 10%  $\text{D}_2\text{O}$ , 100 mM sodium chloride, 10 mM sodium phosphate, and 0.2 mM EDTA.

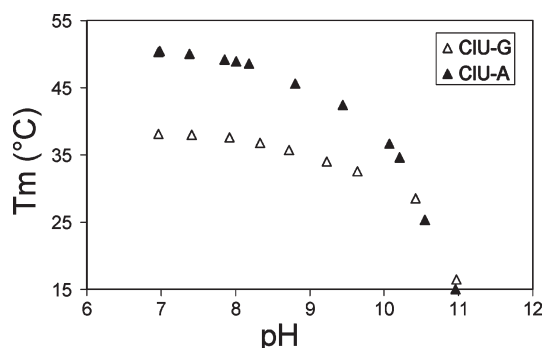


FIGURE 8:  $T_m$  values of CIU-G and CIU-A oligos at different pH values. The values were obtained at a total strand concentration of 6.0  $\mu\text{M}$  in a buffer containing 100 mM sodium chloride, 10 mM sodium phosphate, and 0.1 mM EDTA.

(31, 32) useful in biochemical and pharmacological studies, CIU derivatives and to a lesser extent BrU derivatives could be formed endogenously in the tissue of higher organisms. Derivatives of CIU can be incorporated into the DNA of replicating cells (8–11). Furthermore, CIU has been shown to induce cellular toxicity, cause senescence, and increase the frequency of sister chromatid exchanges (33–36). It has been proposed that the toxicity might, in part, be attributed to interference with nucleotide metabolism, which promotes dUTP misincorporation and repair by a mechanism similar to that proposed for FU (36). However, the mechanism of sister chromatid exchange remains to be resolved.

Recently, we have incorporated CIU into synthetic oligonucleotides to determine its base pairing configuration when paired opposite adenine and to examine the impact of CIU-A substitution on the stability of an oligonucleotide duplex (12). We observed that oligonucleotides containing CIU-A were slightly more stable than the control oligonucleotides containing a T-A base pair. The CIU-A base pair is predominantly in a geometry

that approximates a Watson–Crick base pair, and the duplex containing the CIU-A base pairs was B-form.

In this study, we examined the stability and base pair configuration of a duplex containing a CIU-G mispair (Figure 2). The data obtained were compared with those of a corresponding duplex containing a T-G mispair. The CIU-G duplex has the same thermal stability, within experimental error, as the corresponding T-G duplex. Both mispairs are substantially less stable than the CIU-A duplex (12). Melting temperatures and thermodynamic parameters are listed in Table 1, and representative melting curves are shown in Figure 2.

Proton NMR spectra were recorded for the CIU-G- and T-G-containing duplexes under the same experimental conditions of temperature and neutral pH. The downfield shift of the CIU3 H6 proton relative to the T3 H6 proton by 0.53 ppm is attributed to the opposing inductive properties of the 5-methyl and 5-chloro substituents. A shift similar in magnitude (0.52 ppm) was observed for the corresponding T-A and CIU-A duplexes (12). The nonexchangeable proton connectivities indicate that all bases are intrahelical. The observed chemical shifts of the H6 protons of T3 and CIU3 indicate that the pyrimidines of both the T-G and CIU-G mispairs are predominantly in their neutral, keto tautomeric forms at neutral pH (48).

Exchangeable proton resonances were observed for each base pair in both the T-G and CIU-G duplexes (Figure 4). Two imino proton resonances are observed for each mispair, both shifted upfield from the normal Watson–Crick imino proton region which is characteristic of wobble mispairs (49–51). The exchangeable and nonexchangeable proton NMR data indicate that the bases of both the CIU-G mispair and the T-G mispair are paired with one another in a wobble configuration as shown in Figure 6A.

With an increasing temperature, the exchangeable resonances of the CIU-G mispair broaden rapidly and are lost from the spectrum prior to thermal denaturation of the duplex (Figure 5b and Figures S6 and S7 of the Supporting Information). The rapid broadening of the CIU-G imino protons distinguished the CIU-G and T-G mispairs in that the imino protons of the T-G mispair broaden only as the remainder of the helix is thermally denatured (Figure 5a). The magnitudes of the cross-peaks in our NOESY spectra between the CIU-G imino proton resonances and water are 3–4 times larger than those of the T-G mispair at equal mixing times, suggesting that the enhanced broadening of the CIU-G imino protons occurs by exchange with water (Figure S8 of the Supporting Information). The CIU base of the CIU-G mispair (Figure 6A) could move, allowing the CIU imino proton to be exposed to solvent (Figure 6B). The acidic CIU N3 proton could then exchange with water by ionization of the CIU residue (Figure 6C). The ionized CIU residue could then regain a proton and return to the neutral wobble (Figure 6B to Figure 6A) or remain ionized and form two hydrogen bonds with G (Figure 6D).

A distinguishing feature of CIU, relative to T, is that the 5-chloro substituent of CIU is electron-withdrawing whereas the T methyl group is electron-donating. The electronic-inductive property of a 5-substituted uracil analogue significantly impacts the  $\text{pK}_a$  of the N3 proton. The  $\text{pK}_a$  of CldU is reported to be 7.9, whereas the  $\text{pK}_a$  of the corresponding thymidine N3 proton is 9.7 (19, 21). Previously, both the FU-G (13) and BrU-G (14) mispairs were shown to undergo a pH-dependent structural transition. The  $\text{pK}_a$  of FdU is reported to be 7.7 (19), whereas the  $\text{pK}_a$  when paired with G is 8.3 (13). Similarly, the  $\text{pK}_a$  of BrdU is 8.0 (19), and the  $\text{pK}_a$  of BrU when mispaired with G is 8.6 (14).

We therefore examined the CIU-G duplex as a function of solution pH. As shown in Figure 7 and Figure S11 of the Supporting Information, multiple protons within the duplex undergo pH-dependent changes in chemical shift. The H6 proton of the CIU residue begins to shift upfield, broaden, and is lost from the spectrum by pH 7.9 as it moves beneath other nonexchangeable resonances (Figure S11 of the Supporting Information).

The  $pK_a$  of CIdU is 7.9 (19), whereas the  $pK_a$  in the CIU-G mispair observed here shifted to 8.7. The increase in the apparent  $pK_a$  for CIU when paired opposite G is similar in magnitude for the shifts in  $pK_a$  seen for FU-G and BrU-G discussed above and would correspond to a difference of approximately 1.0 kcal/mol at pH 7.4 and 25 °C (18). The thermal stability of the CIU-A and CIU-G duplexes was examined as a function of solution pH (Figure 8). The observed  $T_m$  for each duplex decreases with increasing solution pH, as would be expected for alkaline-induced denaturation. No unusual pH-dependent change in duplex stability is observed in the region of pH 8.7 for the CIU-G duplex, indicating that the ionized configuration of the CIU-G duplex ( $pK_a = 8.7$ ) does not destabilize the duplex.

Upon the basis of the pH-dependent change from neutral to wobble to ionized pseudo-Watson–Crick configuration, we would anticipate that the base pairing properties of CIU when in DNA would be pH-dependent, which has been demonstrated for the FU and BrU bases (16, 18, 20). As the pH increases, we would anticipate more mispair formation. Several recent studies have indicated that base pair geometry is one of the primary properties that govern base selection by DNA polymerase (52–54). An increased level of miscoding with an increasing pH has been observed for the FU and BrU bases, as well as the thymine oxidation damage product, 5-formyluracil (55). The increased miscoding potential is attributed to an electron-withdrawing substituent in the 5-position (20).

The capacity of a base analogue to induce mutation in a replicating cell would increase with its capacity to miscode but decrease with an increasing efficiency of repair. In vitro systems, both FU and BrU have similar miscoding potential; however, BrU is a known mutagenic base analogue, whereas FU is considered to be only weakly or nonmutagenic. Unlike BrU, FU is repaired by several members of the uracil glycosylase family (21–26). The efficiency of FU repair is attributed to the small size of the 5-substituent and the electron-withdrawing property of the 5-substituent (21–26). Although both bromine and fluorine substituents are electron-withdrawing and induce similar changes in the  $pK_a$  values for the corresponding 5-substituted uracil derivatives, the larger size of the Br substituent prevents its removal by the major uracil glycosylase, UNG.

The repair of CIU is more similar to that of BrU than to that of FU. The CIU analogue is repaired by SMUG1 and TDG, but not UNG. The efficiency of CIU repair is substantially greater when the CIU is mispaired with G than when paired with A (12). The difference in the repair of CIU-A versus CIU-G has been attributed to the reduced stability of the CIU-G mispair. The reduced stability of damaged or mispaired bases appears to be a common recognition mechanism for glycosylases (21–26).

In accord with our previous results with the CIU-A base pair (12), CIU incorporated as a dNTP analogue would be expected to pair predominantly with template A. As a stable base resistant to glycosylase removal (12), CIU-A could be a persistent DNA lesion. When templates containing CIU are replicated, it would potentially miscode with G at a higher

frequency than T because of its increased propensity to form an ionized base pair in pseudo-Watson–Crick geometry, in accord with previous studies with BrU, FU, and 5-formyluracil (16, 55). Once formed, however, the CIU of a CIU-G mispair would be a target for repair by members of the uracil glycosylase family (12). The CIU of the mispair would be targeted for glycosylase removal, leaving the incorrect G in the opposing strand to serve as the template for repair synthesis. On the basis of these properties, the formation of CIU in the nucleotide pool could prove to be highly mutagenic.

## SUPPORTING INFORMATION AVAILABLE

Additional experimental data, including two tables of NMR chemical shifts, the mass spectral characterization of the CIU-G oligonucleotide, and 10 figures showing 1D and 2D NMR spectra. This material is available free of charge via the Internet at <http://pubs.acs.org>.

## REFERENCES

1. Henderson, J. P., Byun, J., Takeshita, J., and Heineke, J. W. (2003) Phagocytes produce 5-chlorouracil and 5-bromouracil, two mutagenic products of myeloperoxidase, in human inflammatory tissue. *J. Biol. Chem.* 278, 23522–23528.
2. Jiang, Q., Blount, B. C., and Ames, B. N. (2003) 5-Chlorouracil, a marker of DNA damage from hypochlorous acid during inflammation: A gas chromatography-mass spectrometry assay. *J. Biol. Chem.* 278, 32834–32840.
3. Takeshita, J., Byun, J., Nhan, T. Q., Pritchard, D. K., Pennathur, S., Schwartz, S. M., Chait, A., and Heineke, J. W. (2006) Myeloperoxidase generates 5-chlorouracil in human atherosclerotic tissue: A potential pathway for somatic mutagenesis by macrophages. *J. Biol. Chem.* 281, 3096–3104.
4. Knaapen, A. M., Güngör, N., Schins, R. P., Borm, P. J., and Van Schooten, F. J. (2006) Neutrophils and respiratory tract DNA damage and mutagenesis: A review. *Mutagenesis* 21, 225–236.
5. Whiteman, M., Jenner, A., and Halliwell, B. (1997) Hypochlorous acid-induced base modifications in isolated calf thymus DNA. *Chem. Res. Toxicol.* 10, 1240–1246.
6. Valinluck, V., and Sowers, L. C. (2007) Inflammation-mediated cytosine damage: A mechanistic link between inflammation and the epigenetic alterations in human cancers. *Cancer Res.* 67, 5583–5586.
7. Kang, J. I., and Sowers, L. C. (2008) Examination of hypochlorous acid-induced damage to cytosine residues in a CpG dinucleotide in DNA. *Chem. Res. Toxicol.* 21, 1211–1218.
8. Visser, D. W., Frisch, D. M., and Huang, B. (1960) Synthesis of 5-chlorodeoxyuridine and a comparative study of 5-halodeoxyuridines in *E. coli*. *Biochem. Pharmacol.* 5, 157–164.
9. Jaunin, F., Visser, A. E., Cmarko, D., Aten, J. A., and Fakan, S. (1998) A new immunocytochemical technique for ultrastructural analysis of DNA replication in proliferating cells after application of two halogenated deoxyuridine. *J. Histochem. Cytochem.* 46, 1203–1209.
10. Svetlova, M., Solovjeva, L., Blasius, M., Shevelev, I., Hubscher, U., Hanawalt, P., and Tomilin, N. (2005) Differential incorporation of halogenated deoxyuridines during UV-induced DNA repair synthesis in human cells. *DNA Repair* 4, 359–366.
11. Yamada, K., Semba, R., Ding, X., Ma, N., and Nagahama, M. (2005) Discrimination of cell nuclei in early S-phase, mid-to-late S-phase, and G2/M-phase by sequential administration of 5-bromo-2'-deoxyuridine and 5-chloro-2'-deoxyuridine. *J. Histochem. Cytochem.* 53, 1365–1370.
12. Theruvathu, J. A., Kim, C. H., Rogstad, D. K., Neidigh, J. W., and Sowers, L. C. (2009) Base-pairing configuration and stability of an oligonucleotide duplex containing a 5-chlorouracil-adenine base pair. *Biochemistry* 48, 7539–7546.
13. Sowers, L. C., Eritja, R., Kaplan, B., Goodman, M. F., and Fazakerley, G. V. (1988) Equilibrium between a wobble and ionized base pair formed between fluorouracil and guanine in DNA as studied by proton and fluorine NMR. *J. Biol. Chem.* 263, 14794–14801.
14. Sowers, L. C., Goodman, M. F., Eritja, R., Kaplan, B., and Fazakerley, G. V. (1989) Ionized and wobble base-pairing for bromouracil-guanine equilibrium under physiological conditions. A nuclear

- magnetic resonance study on an oligonucleotide containing a bromouracil-guanine base-pair as a function of pH. *J. Mol. Biol.* 205, 437–447.
15. Brown, T., Kneale, G., Hunter, W. N., and Kennard, O. (1986) Structural characterization of the bromouracil-guanine base pair mismatch in a Z-DNA fragment. *Nucleic Acids Res.* 14, 1801–1809.
  16. Yu, H., Eritja, R. E., Bloom, L. B., and Goodman, M. F. (1993) Ionization of bromouracil and fluorouracil stimulates base mispairing frequencies with guanine. *J. Biol. Chem.* 268, 15935–15943.
  17. Lawley, P. D., and Brookes, P. (1962) Ionization of DNA bases or base analogs as a possible explanation of mutagenesis with special reference to 5-bromodeoxyuridine. *J. Mol. Biol.* 4, 216–219.
  18. Sowers, L. C., Shaw, B. R., Veigl, M. L., and Sedwick, W. D. (1987) DNA base modification: Ionized base pairs and mutagenesis. *Mutat. Res.* 177, 201–218.
  19. La Francois, C. J., Jang, Y. H., Cagin, T., Goddard, W. A.III, and Sowers, L. C. (2000) Conformation and proton configuration of pyrimidine deoxynucleoside oxidation damage products in water. *Chem. Res. Toxicol.* 13, 462–470.
  20. Privat, E. J., and Sowers, L. C. (1996) A proposed mechanism for the mutagenicity of 5-formyluracil. *Mutat. Res.* 354, 151–156.
  21. Liu, P., Burdzy, A., and Sowers, L. C. (2002) Substrate recognition by a family of uracil-DNA glycosylases: UNG, MUG and TDG. *Chem. Res. Toxicol.* 15, 1001–1009.
  22. Liu, P., Burdzy, A., and Sowers, L. C. (2003) Repair of the Mutagenic DNA oxidation product, 5-formyluracil. *DNA Repair* 2, 199–210.
  23. Bennett, M. T., Rodgers, M. T., Hebert, A. S., Ruslander, L. E., Eisele, L., and Drohat, A. C. (2006) Specificity of human thymine DNA glycosylase depends on N-glycosidic bond stability. *J. Am. Chem. Soc.* 128, 12510–12519.
  24. Morgan, M. T., Bennett, M. T., and Drohat, A. C. (2007) Excision of 5-halogenated uracils by human thymine DNA glycosylase. Robust activity for DNA contexts other than CpG. *J. Biol. Chem.* 282, 27578–27586.
  25. Liu, P., Theruvathu, J. A., Darwanto, A., Lao, V. V., Pascal, T., Goddard, W. A.III, and Sowers, L. C. (2008) Mechanism of base selection by the *Escherichia coli* mispaired uracil glycosylase. *J. Biol. Chem.* 283, 8829–8836.
  26. Darwanto, A., Theruvathu, J. A., Sowers, J. L., Rogstad, D. K., Pascal, T., Goddard, W. A.III, and Sowers, L. C. (2009) Mechanism of base selection by human single-stranded selective monofunctional uracil-DNA-glycosylase. *J. Biol. Chem.* 284, 15835–15846.
  27. Parker, W. B., and Cheng, Y. C. (1990) Metabolism and mechanism of action of 5-fluorouracil. *Pharmacol. Ther.* 48, 381–395.
  28. Wyatt, M. D., and Wilson, D. M.III (2009) Participation of DNA repair in the response to 5-fluorouracil. *Cell. Mol. Life Sci.* 66, 788–799.
  29. Sternglanz, H., and Bugg, C. E. (1975) Relationship between the mutagenic and base-stacking properties of halogenated uracil derivatives. The crystal structure of 5-chloro- and 5-bromouracil. *Biochim. Biophys. Acta* 378, 1–11.
  30. Henderson, J. P., Byun, J., Mueller, D. M., and Heinecke, J. W. (2001) The eosinophil peroxidase-hydrogen peroxide-bromide system of human eosinophils generates 5-bromouracil, a mutagenic thymine analog. *Biochemistry* 40, 2052–2059.
  31. Brennan, C. A., Van Cleve, M. D., and Gumport, R. I. (1986) The effects of base analogue substitutions on the cleavage by the EcoRI restriction endonuclease of octadeoxyribonucleotides containing modified EcoRI recognition sequences. *J. Biol. Chem.* 261, 7270–7278.
  32. Petruska, J., and Horn, D. (1983) Sequence-specific responses of restriction endonucleases to bromodeoxyuridine substitution in mammalian DNA. *Nucleic Acids Res.* 11, 2495–2510.
  33. Morris, S. M. (1993) The genetic toxicology of 5-fluoropyrimidines and 5-chlorouracil. *Mutat. Res.* 297, 39–51.
  34. Michishita, E., Kurahashi, T., Suzuki, T., Fukuda, M., Fujii, M., Hirano, H., and Ayusawa, D. (2002) Changes in nuclear matrix proteins during senescence-like phenomenon induced by 5-chlorodeoxyuridine in HeLa cells. *Exp. Gerontol.* 37, 885–890.
  35. Heartlein, M. W., O'Neill, J. P., Pal, B. C., and Preston, R. J. (1982) The induction of specific-locus mutations and sister-chromatid exchanges by 5-bromo- and 5-chloro-deoxyuridine. *Mutat. Res.* 92, 411–416.
  36. Brandon, M. L., Mi, L.-J., Chaung, W., Teebor, G., and Boorstein, R. J. (2000) 5-Chloro-2'-deoxyuridine cytotoxicity results from base excision repair of uracil subsequent to thymidylate synthase inhibition. *Mutat. Res.* 459, 161–169.
  37. Kumar, R., Wiebe, L. I., and Knaus, E. E. (1994) A mild and efficient methodology for the synthesis of 5-halogeno uracil nucleosides that occur via a 5-halogeno-6-azido-5,6-dihydro intermediate. *Can. J. Chem.* 72, 2005–2010.
  38. Cui, Z., Theruvathu, J. A., Farrel, A., Burdzy, A., and Sowers, L. C. (2008) Characterization of synthetic oligonucleotides containing biologically important modified bases by matrix-assisted laser desorption time-of-flight mass spectrometry. *Anal. Biochem.* 379, 196–207.
  39. Kang, J. I.Jr., Burdzy, A., Liu, P., and Sowers, L. C. (2004) Synthesis and characterization of oligonucleotides containing 5-chlorocytosine. *Chem. Res. Toxicol.* 17, 1236–1244.
  40. Breslauer, K. J., Frank, R., Blocker, H., and Marky, L. A. (1986) Predicting DNA duplex stability from base sequence. *Proc. Natl. Acad. Sci. U.S.A.* 83, 3746–3750.
  41. SantaLucia, J.Jr., Allawi, H. T., and Seneviratne, P. A. (1996) Improved nearest-neighbor parameters for predicting DNA duplex stability. *Biochemistry* 35, 3555–3562.
  42. Allawi, H. T., and SantaLucia, J.Jr. (1997) Thermodynamics and NMR of internal G·T mismatches in DNA. *Biochemistry* 36, 10581–10594.
  43. Patel, D. J., Kozlowski, S. A., Marky, L. A., Broka, C., Rice, J. A., Itakura, K., and Breslauer, K. J. (1982) Premelting and melting transitions in the d(CGCGAATTCGCG) self-complementary duplex in solution. *Biochemistry* 21, 428–436.
  44. Hare, D. R., Wemmer, D. E., Chou, S. H., Drobny, G., and Reid, B. R. (1983) Assignment of the non-exchangeable proton resonances of d(C-G-C-G-A-A-T-T-C-G-C-G) using two-dimensional nuclear magnetic resonance methods. *J. Mol. Biol.* 171, 319–336.
  45. Klevit, R. E., Wemmer, D. E., and Reid, B. R. (1986) <sup>1</sup>H NMR studies on the interaction between distamycin A and a symmetrical DNA dodecamer. *Biochemistry* 25, 3296–3303.
  46. Liu, M. L., Mao, X. A., Ye, C. H., Huang, H., Nicholson, J. K., and Lindon, J. C. (1998) Improved WATERGATE Pulse Sequences for Solvent Suppression in NMR Spectroscopy. *J. Magn. Reson.* 132, 125–129.
  47. Weiss, M. A., Patel, D. J., Sauer, R. T., and Karplus, M. (1984) Two-dimensional <sup>1</sup>H NMR study of the lambda operator site OL1: A sequential assignment strategy and its application. *Proc. Natl. Acad. Sci. U.S.A.* 81, 130–134.
  48. Sowers, L. C., Fazakerley, G. V., Kim, H., Dalton, L., and Goodman, M. F. (1986) Variation of nonexchangeable proton resonance chemical shifts as a probe of aberrant base pair formation in DNA. *Biochemistry* 25, 3983–3988.
  49. Patel, D. J., Kozlowski, S. A., Marky, L. A., Rice, J. A., Broka, C., Dallas, J., Itakura, K., and Breslauer, K. J. (1982) Structure, dynamics and energetics of deoxyguanosine-thymidine wobble base pair formation in the self-complementary d(CGTAATTCGC) duplex in solution. *Biochemistry* 21, 437–444.
  50. Carbonnaux, C., Fazakerley, G. V., and Sowers, L. C. (1990) An NMR study of deaminated base pairs in DNA. *Nucleic Acids Res.* 18, 4075–4081.
  51. Pardi, A., Morden, K. M., Patel, D. J., and Tinoco, I.Jr. (1982) Kinetics for exchange of imino protons in the d(C-G-C-A-A-T-T-C-G-C-G) double helix and in two similar helices that contain a G-T base pair, d(C-G-T-G-A-A-T-T-C-G-C-G), and an extra adenine, d(C-G-C-A-G-A-A-T-T-C-G-C-G). *Biochemistry* 21, 6567–6574.
  52. Delaney, J. C., Henderson, P. T., Helquist, S. A., Morales, J. C., Essigmann, J. M., and Kool, E. T. (2003) High-fidelity in vivo replication of DNA base shape mimics without hydrogen bonds. *Proc. Natl. Acad. Sci. U.S.A.* 100, 4469–4473.
  53. Goodman, M. F. (1999) On the wagon-DNA polymerase joins “H-bonds anonymous”. *Nat. Biotechnol.* 17, 640–641.
  54. Goodman, M. F. (1997) Hydrogen bonding revisited: Geometric selection as a principle determinant of DNA replication fidelity. *Proc. Natl. Acad. Sci. U.S.A.* 94, 10493–10495.
  55. Yoshida, M., Makino, K., Morita, H., Terato, H., Ohya, Y., and Ide, H. (1997) Substrate and mispairing properties of 5-formyl-2'-deoxyuridine 5'-triphosphate assessed by in vitro DNA polymerase reactions. *Nucleic Acids Res.* 25, 1570–1577.